Structure-Based Design, Synthesis, and Antimicrobial Activity of Indazole-Derived SAH/MTA Nucleosidase Inhibitors

Xiaoming Li,[§] Sam Chu,[§] Victoria A. Feher,[†] Mitra Khalili,[§] Zhe Nie,[§] Stephen Margosiak,[‡] Victor Nikulin,[§] James Levin,[||] Kelly G. Sprankle,[§] Martina E. Tedder,[§] Robert Almassy,[†] Krzysztof Appelt, and Kraig M. Yager*,[§]

Departments of Medicinal Chemistry, Protein Biochemistry, and Structural Biology, Quorex Pharmaceuticals, Carlsbad, California 92008

Received April 29, 2003

The structure-based design, synthesis, and biological activity of a novel indazole-containing inhibitor series for *S*-adenosyl homocysteine/methylthioadenosine (SAH/MTA) nucleosidase are described. Use of 5-aminoindazole as the core scaffold provided a structure-guided series of low nanomolar inhibitors with broad-spectrum antimicrobial activity. The implementation of structure-based methodologies provided a 6000-fold increase in potency over a short timeline (several months) and an economy of synthesized compounds.

Introduction

Growing drug resistance among bacterial pathogens drives the need for new agents effective against them. Ideally, such antibacterial agents hit essential proteins that (i) appear in as many bacterial pathogens as possible but (ii) differ significantly from related mammalian proteins, to yield a broad spectrum of activity with minimal mechanism-based toxicity.

S-adenosyl homocysteine/methylthioadenosine (SAH/MTA) nucleosidase presents a potentially useful target, for three reasons. First, as a product of the highly conserved *pfs* gene,[1] its active site is similarly highly conserved across bacterial species, while differing from that of the related mammalian proteins (methylthioadenosine phosphorylase and purine nucleotide phosphorylase[2,3]). Second, SAH/MTA nucleosidase participates in synthesis of the quorum sensing autoinducer AI-2,[4] which in turn stimulates expression of virulence factors. Consequently, inhibiting SAH/MTA nucleosidase should attenuate bacterial virulence. Third, and most importantly, such inhibition should kill bacteria because accumulation of SAH and MTA inhibits certain essential methyltransferase reactions and thereby impedes recycling of adenine and methionine (necessary for DNA and protein synthesis, respectively) (Figure 1).

These features provide an enzyme target well-suited for structure-based design of a broad-spectrum antibacterial drug with low potential for mechanism-based toxicity in mammals. We describe here the rationale and results of this approach.

In Silico Lead Identification

Selection of compounds for screening in the SAH/MTA nucleosidase activity assay began by filtering a virtual library of ~390 000 commercially available compounds to approximately 2000 satisfying the following criteria: (i) possessing three pharmacophoric features identified from inspection of homology model: substrate complexes, (ii) having molecular volumes less than that of the homology model binding pocket, and (iii) conforming to Lipinski[5] guidelines (i.e., molecular weight < 500, $-2.0 < C_{logP} < 5.0$). The resulting data set was clustered for 2D fingerprint diversity and a representative selection of 1288 compounds identified using SELECTOR (Tripos, Inc.).

X-ray structural determination of lead compounds cocrystallized with SAH/MTA nucleosidase derived from *Escherichia coli* and other pathogenic species revealed the mode of inhibitor binding within the active site. These co-structures provided the structural information for design of individual compounds and focused libraries.

Chemical Methods

Syntheses of substituted indazole SAH/MTA nucleosidase inhibitors began from commercially available 5-nitroindazole (**1**) and from 2-chloro-5-nitro acetophenone (**2**) (Scheme 1). A solution of **1** in glacial AcOH was exposed to chlorine gas providing 3-chloroindazole (**3**) in good yield.[6] Condensation of acetophenone **2** with hydrazine afforded the corresponding 3-methyl derivative **4**. Reduction of the nitro groups either by hydrogenation over palladium or, in the case of the 3-chloro derivative **3**, by heating with an excess of stannous chloride, avoided complications due to over-reduction and loss of the 3-chloro substituent. Regardless of method, the crude amino indazoles were typically used without further purification and were allowed to react with desired sulfonyl chlorides. Initial attempts to selectively sulfonylate the C5 and C6 amino groups over the indazole N1 nitrogen were problematic. Ultimately, by using pyridine as both the base and the solvent, we were able to cleanly and reproducibly modify only the C5 and C6 amino groups.

Synthesis of 3,5,7-trisubstituted indazoles (Scheme 2) began with nitration of 3 and 4 to provide 5,7-dinitroindazoles **10** and **11** in good yield.[7] Treatment with aqueous ammonium sulfide[8] cleanly and selectively reduced the 7- but not the 5-NO₂ group to provide the 7-amino-5 nitro indazoles **12** and **13**. Initial attempts to protect the C7 amino group, sulfonylate C5, and

* To whom correspondence should be addressed. Quorex Pharmaceuticals, 1890 Rutherford Drive, Carlsbad, CA 92008. Phone: (760) 494−6230. Fax (760) 602−1915. E-mail: kyager@quorex.com.
§ Department of Medicinal Chemistry.
‡ Department of Protein Biochemistry.
† Department of Structural Biology.
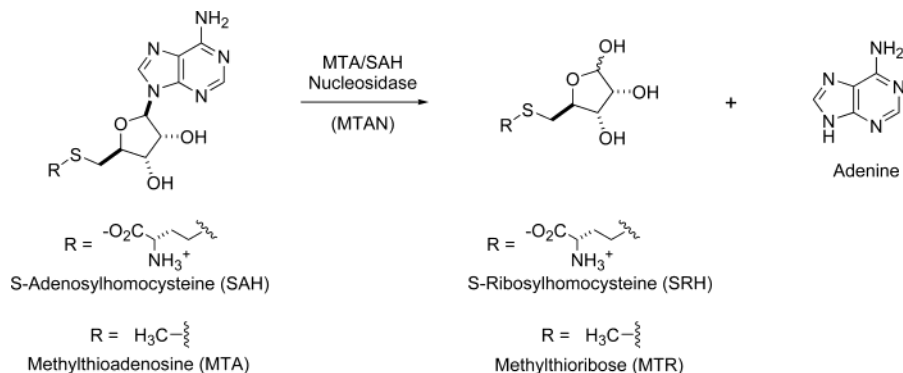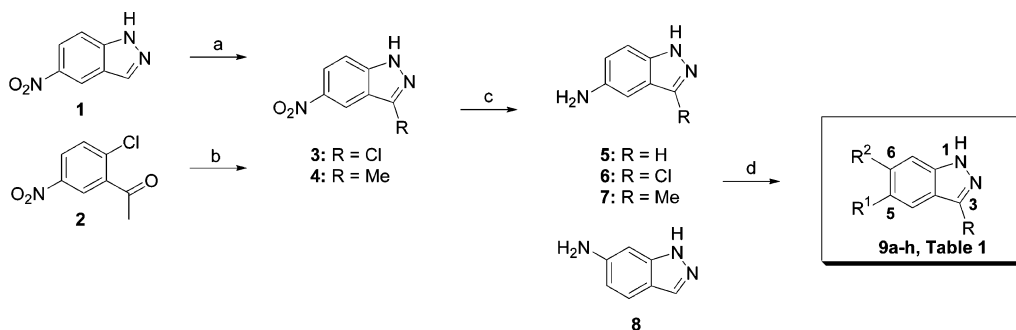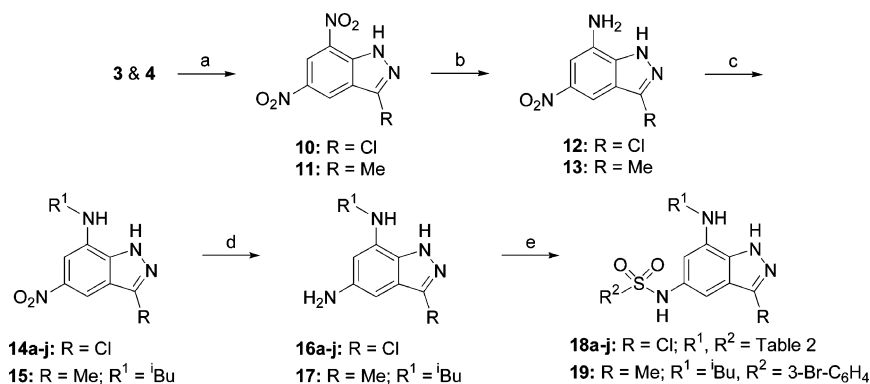|| Department of Preclinical Microbiology.

Figure 1. Reaction catalyzed by MTA nucleosidase in vivo.

Scheme 1[a]

[a] Reagents: (a) Cl₂, AcOH; (b) H₂NNH₂, DMF; (c) SnCl₂, EtOH or H₂, Pd/C, MeOH; (d) dansyl chloride or 4-chlorobenzenesulfonyl chloride, pyr.

Scheme 2[a]

[a] Reagents: (a) HNO₃, H₂SO₄; (b) S(NH₄)₂, EtOH; (c) R¹CHO, NaBH(OAc)₃, THF; (d) SnCl₂, EtOH or H₂, Pd/C, MeOH; (e) R²SO₂Cl, pyr.

deprotect the C7 amino group failed due to the proximity of the latter to the N1 secondary amino group. Ultimately, reductive amination[9] with an appropriate aldehyde followed by reduction of the C5 nitro group and sulfonylation afforded aliphatic and aryl aliphatic groups at the C7 position (Scheme 2). Less reactive aldehydes necessitated either reaction with the indazole prior to reduction with NaBH(OAc)₃, or introduction of the aldehyde portionwise during the reaction, to minimize consumption of the aldehyde by the reducing agent. This approach, albeit tedious, proved effective and allowed optimization of interactions between the enzyme and the C7 substituent of the inhibitors.

The more highly elaborated C5 biphenyl sulfonamides were incorporated by direct sulfonylation in pyridine when the sulfonyl chloride was available, or by Suzuki[10] type palladium-mediated arylation of bromo sulfamides **18k** and **19** with commercially or synthetically derived aryl boronates (Scheme 3).

Biological Methods

In a primary screen for SAH/MTA nucleosidase inhibition, homocysteine from cleavage of residual *S*-adenosyl homocysteine by SAH hydrolase was determined spectrophotometrically (at 405 nm) by monitoring the 2-nitro-4-mercaptobenzoate generated upon addition of 5,5′-dithiobis(2-nitrobenzoic acid) (DTNB). Addition of adenosine deaminase to assay mixtures removed the inhibitory SAH/MTA nucleosidase product, adenine, and thereby ensured rapid SAH turnover. A secondary assay monitored the turnover of MTA by SAH/MTA nucleosidase directly as the loss of MTA peak area in an HPLC chromatogram.

Results and Discussion

The co-structure of **9a** with SAH/MTA nucleosidase confirmed the binding mode predicted by docking inhibitors into the enzyme active site (Figure 2). Key

Scheme 3[a]
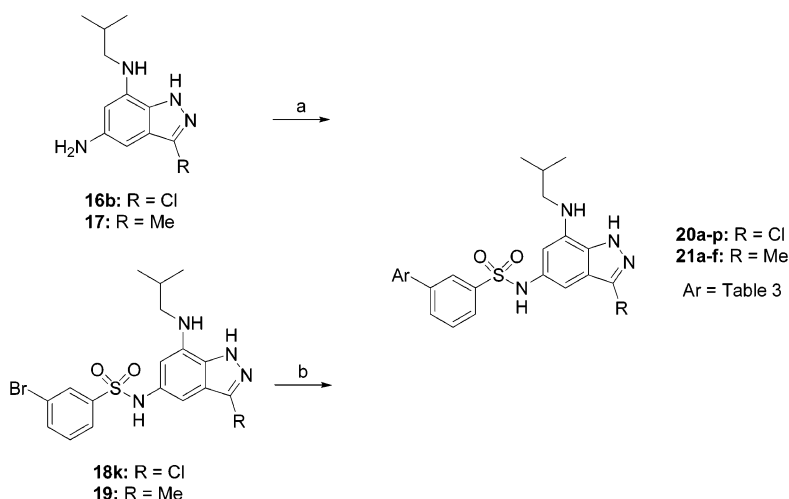
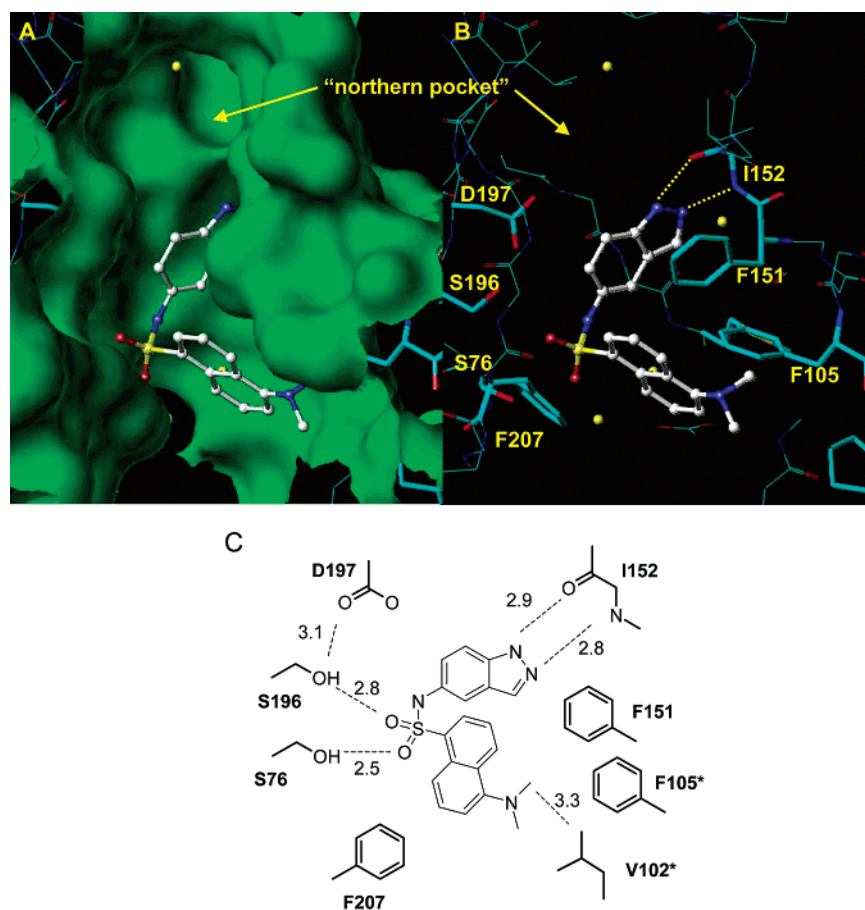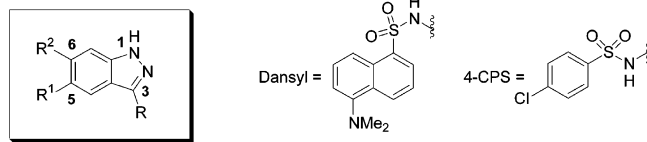[a] Reagents: (a) 3-Ar-C$_6$H$_4$SO$_2$Cl, pyr.; (b) ArB(OR^3)$_2$, Pd(PPh$_3$)$_4$, aq. Na$_2$CO$_3$, DME.

Figure 2. Compound **9a** (K_i = 2.8 μM) bound in the active site of SAH/MTA nucleosidase as determined by X-ray crystallography. The solvent-accessible surface of the active site (A) illustrates the general shape of the pocket. The hydrogen bonding pattern comprised of protein backbone and side-chain interactions are illustrated in (B, C). Inhibitor hydrophobic interactions with a cluster of phenylalanines and V102 are also illustrated; residues from the associated monomer are indicated by an asterisk (C). Bound water molecules are indicated as yellow spheres (A, B).

features of the binding include those observed in the adenine:SAH/MTA nucleosidase cocrystal structure[1e]: a pair of hydrogen bonds between the heterocyclic core of the inhibitor and I152 and edge-on π−π interactions with F151 (⟨dist⟩ = 4.0 Å). Here N1 of the inhibitor donates a hydrogen bond to the carbonyl oxygen atom of I152 while N2 accepts a hydrogen bond from the I152 backbone NH. Additional hydrogen bonding interactions between the sulfonamide oxygen atoms and two serine

residues S76 and S196 further stabilize the inhibitor−enzyme complex. The dansyl group makes a series of hydrophobic interactions: a staggered π−π stacking interaction with F207 (⟨dist⟩ = 4.1 Å), a face-on π−π stacking interaction with F105 (⟨dist⟩ = 4.0 Å), and a van der Waals contact between the methylamine and V102; these latter two residues are contributed from the neighboring monomer. Ab initio methods predict that the cisoid sulfonamide bond geometries observed in the

Table 1. Inhibitors of SAH/MTA Nucleosidase: Relative and Absolute Affects of Substituents at C3, C5, and C6

Dansyl =

4-CPS =

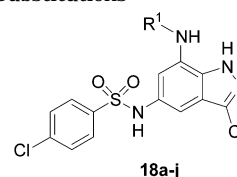| compound **9**	R	R^1	R^2	K_i (μM)
a	H	dansyl	H	2.8
b	H	H	dansyl	1
c	Cl	dansyl	H	22
d	Me	dansyl	H	64
e	H	4-CPS	H	27
f	H	H	4-CPS	17
g	Cl	4-CPS	H	5.2
h	Me	4-CPS	H	4

crystal structure are among the lowest energy conformers; thus there is not a significant energy penalty for the compound to adopt the observed conformer. Interestingly, despite the bulk of the dansyl group, moving it from the 6- to the 5-position (as in **9b** to **9a**) has little effect on potency, as long as the 3-position remains unsubstituted. Apparently 180° rotation about the C(aryl)-N(sulfonamide) bond of **9a** and a slight upward shift within the pocket allows hydrogen bonding and favorable hydrophobic interactions comparable with those of **9b** (binding as the 2H-indazole tautomer).
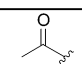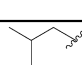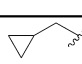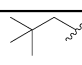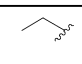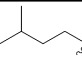
Substituents on the 3-position, however, preclude this accommodation in 5-dansyl derivatives **9c** (3-Cl) and **9d** (3-Me). Movement to mitigate the steric bulk of their 5-dansyl groups forces their 3-substituents too close to the protein backbone. As a consequence, 3-substituted derivatives **9c** and **9d** bind poorly (K_i = 22 and 64 μM, respectively).

Replacing the 5-dansyl substituent with the lesser sterically demanding 4-chlorophenylsulfonamide group, however, largely restores activity in the 3-Cl and 3-Me derivatives **9g** and **9h**. Importantly, this replacement therefore allows functionalization at C3 to address, e.g., metabolism issues that might otherwise arise from the presence of a hydrogen atom at this position.

Examination of the **9a**·MTA nucleosidase co-structure revealed a hydrophobic pocket (referred to as the "northern pocket") adjacent to the 1- and 6-positions of **9a** (Figure 2) that, although highly conserved, does not participate in binding the native substrate. A suitably designed inhibitor could therefore exploit this "northern pocket" to improve its binding to the bacterial enzyme not only in an absolute sense (increasing its potency against bacteria), but also in a relative sense *vis a vis* mammalian analogues (increasing its selectivity for the bacterial enzyme and thereby minimizing its mechanism-based toxicity in mammals).

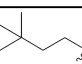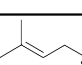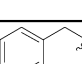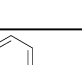Initial attempts to access the "northern pocket" with the 7-acetamide derivative **18a** (Scheme 2) decreased inhibition activity 2-fold with respect to the 7-unsubstituted derivative **9g** (Table 2). The structure of **18a** bound to MTA nucleosidase suggested that the relatively poor affinity arose from a dramatic 1.6 Å upward shift of inhibitor within the active site compared to the position of bound **9a** (Figure 3). This shift allows the relatively small active site side pocket to accommodate the larger C7-chloro group. Furthermore, this upward

Table 2. Trisubstituted Indazole Inhibitors of SAH/MTA Nucleosidase: C7 Substitutions

18a-j

Compound **18**	R^1	K_i (μM)	$\Delta G°_{solvn}$ (kcal/mol)[a]
a		11	-19.5
b		0.76	-15.1
c		0.5	-15.3
d		1.2	-14.4
e		2.7	-16.1
f		4.9	-14.4
g		6.5	-14.1
h		2.2	-14.5
i		1.8	-15.6
j		2.3	-16.4

[a] $\Delta G°$ solvation energies determined using SE-AM1 methods and the Cramer/Truhlar 5.4 model[12] in Spartan (Wavefunction, Inc.). Compound conformations were generated by minimizing each compound in the protein active site or by relaxing the cocrystal ligand structures. The mean value for compounds **18b**−**18j** is 15.1 ± 1.0 kcal/mol.

shift within the active site pocket allows the inhibitor to make a more direct face on $\pi-\pi$ stacking interaction between the 4-chlorophenyl group of **18a** and the side-chain phenyl of F207. The crystal structure illustrates a second reason for the poor affinity of this inhibitor (Figure 4). The orientation of the C7 acetyl group toward the hydrophobic "northern" pocket clearly failed to maximize favorable interactions. While the C7 amide NH hydrogen bonds with the side-chain carboxyl group of D197, formation of an internal hydrogen bond between the acetyl carbonyl oxygen atom and N1 brings the former unfavorably close to the backbone carbonyl group of I152 (dist. = 2.9 Å). Reduction of the C7
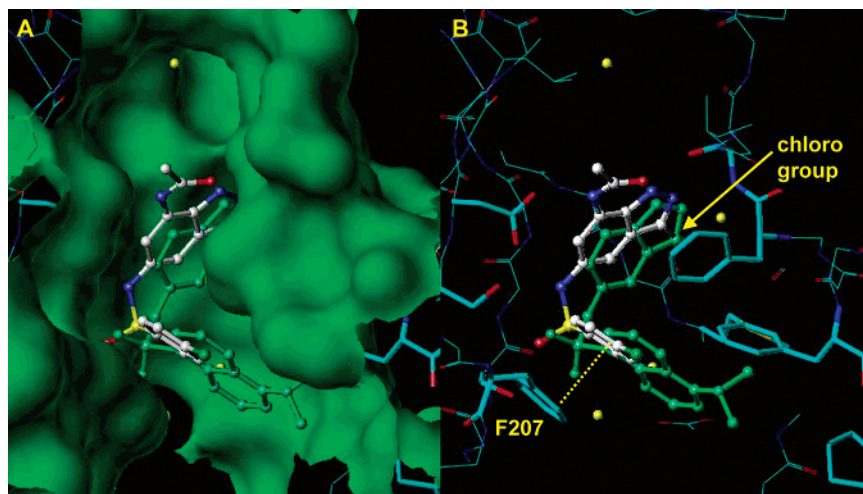
Figure 3. Superposition of **9a** (blue-green) and **18a** (atom-type color) cocrystal structures illustrating the 1.6 Å upward shift of **18a** within the active site to accommodate the C3 chloro group in the small side pocket. The solvent-accessible surface is included (A) to outline the overall shape of the protein active site represented as stick in (B).
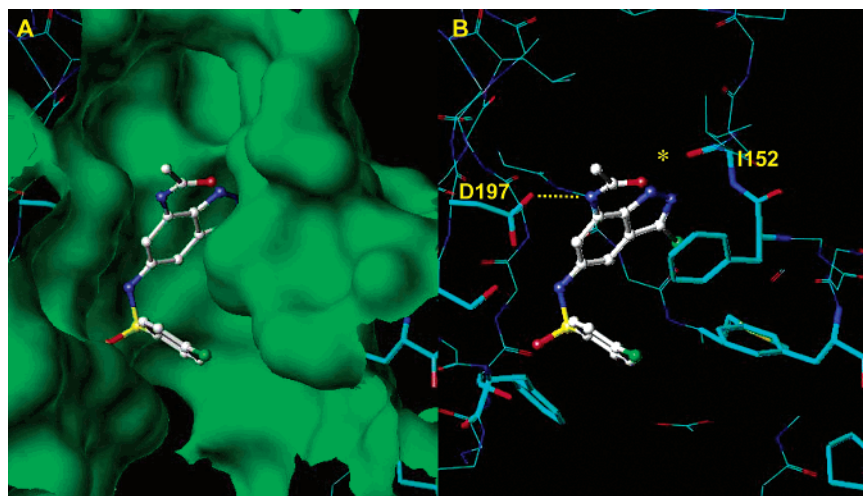

Figure 4. Compound **18a** ($K_i = 11.0\ \mu$M) in the SAH/MTA nucleosidase active site as determined by X-ray crystallography. This derivative has a chloro group at C3 and an acetamide at the C7-positions of the indazole core. The acetamide N is 2.9 Å from the D197 Oγ. The intramolecular hydrogen bond between the acetamide carbonyl group and the N1 hydrogen places the former within 3.0 Å of I152 carbonyl creating an unfavorable (denoted with an asterisk) contact. The binding mode for **18a** establishes direct $\pi-\pi$ stacking of the 4-chlorophenyl and F207 ($\langle$dist$\rangle$ = 3.55 Å). The solvent-accessible surface is included (A) to outline the overall shape of the protein active site in stick representation (B).

acetamide group to the corresponding ethylamino group (to yield **18e**) eliminated this contact and thereby improved potency 2-fold. This change also is favored by relative desolvation energies for these two compounds.

The next objective was to find the C7 substituent that best occupied the hydrophobic space afforded by the enzyme's northern pocket. The volume of this pocket varies dramatically from completely occluded in the formycin-MTA nucleosidase structure to a solvent-accessible one in the adenine-MTA nucleosidase structure. This variation complicated modeling predictions for the appropriate substituents at C7 and necessitated a more traditional approach to establish the structure–activity relationship. Results for relatively large aromatic groups, cf. **18i** and **18j**, and a variety of small, branched, unsaturated, and cyclic aliphatic groups as C7 substituents show that the larger aliphatic and aromatic substituents are not accommodated in the pocket as well as the smaller substituents (Table 2). Although this may be a consequence of the relative solvation energies (perhaps contributing ∼1 kcal/mol for

the aryl substitutions), the uncertainties in the calculated values are on the same order as the differences between $\Delta G^{\circ}_{\text{solvation}}$ for these compounds over this limited K_i range (Table 2). The results are best understood as demonstrating limitations in the size and shape of the pocket, the ability of the flexible loop to accommodate these compounds, and limits in the conformational energies required for these compounds to adopt the bound shape. Overall, the isobutyl and cyclopropylmethyl derivatives **18b** ($K_i = 760$ nM) and **18c** ($K_i = 500$ nM), offered the best activity ($K_i = 760$ and $K_i = 500$ nM, respectively).

With the indazole core optimized, attention turned to other sites for potentially improving binding affinities. In the cocrystal structure for **18b**, a hydrophobic channel near the dimer interface is observed that flanks the area occupied by the 4-chlorophenyl group (Figure 5). An appropriately substituted aryl sulfonamide could fill this relatively solvent-accessible space, and X-ray structure analysis suggested that the 3-position of the aryl sulfonamide offered the most promising way of accessing
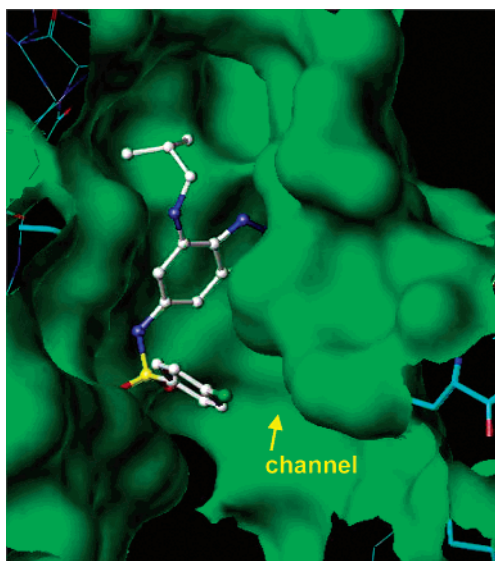
Figure 5. The solvent-accessible surface (green) for the active site cocrystal structure with **18b** (K_i = 0.76 μM) illustrates the replacement of the acetyl group at the C7 NH indazole position. This hydrophobic substituent better fits into the "northern pocket" and removes the intramolecular hydrogen bond observed in **18a**. The channel to the right of the 4-chlorophenyl group is indicated (see text).

this channel. It was also clear that an additional arene directly linked to this position would yield maximal interaction. The first meta-biphenyl derivative prepared (**20b**, with a 4-chlorophenyl group meta to the sulfonamide linkage, Table 3) provided gratifying confirmation of this suggestion by improving binding approximately 60-fold.

A co-structure of **20f** with the enzyme confirmed this binding hypothesis (Figure 6). The hydrophobic residues F105, F151, V102, P113, and M173 together form the channel and provide key contacts between the inhibitor and protein. The interaction between F151 and the inhibitor appears to be especially important. Here, as in earlier inhibitor–protein complexes, staggered $\pi-\pi$ stacking interaction ($\langle$dist$\rangle$ = 4.0 Å) between the indazole core and the phenyl ring of F151 in combination with a $\pi-\sigma$ interaction with the proximal arene of the biarylsulfonamide should promote binding of these and all the 4-chlorophenylsulfonamide derivatives. However, in the case of the biaryl analogues, additional affinity (10–475-fold) results from $\pi-\pi$ stacking of the distal arene, in this case, the pyrimidine ring with the phenyl group of F105. This key interaction essentially locks the inhibitor in the active site. Substitution on the distal arene yields two benefits: small groups in the meta position occupy a small cavity created by the side-chains of M173, V102, and P113 and provide ca. 2–3-fold additional affinity, while halogens in this and other positions on the distal arene withdraw electron density from this and proximal arene, which, from the derived SAR, appears to promote favorable ligand–protein interactions. The dihedral angle of the biaryl system in bound **20f** (32.7°; cf. the theoretically and empirically expected angle of 50–60°) allows maximal $\pi-\pi$ interaction with F105 without perturbing the edge-on interaction between F151 and F105. Mitigation of the energetic penalties for this dihedral angle may further improve the binding of these inhibitors.

Antibacterial Activity. Determination of minimum inhibitory concentrations for several Gram-positive and -negative pathogenic bacteria showed that the most potent inhibitor (**20c**; K_i = 1.6 nM) has modest activity against the Gram-negative bacterium *Neisseria meningitidis* but little against Gram-positive strains. Compounds **20a** and **20b** yielded the broadest spectrum of activity, showing comparable, albeit unexceptional, activity against both Gram-positive and -negative organisms. These and other indazole derivatives have antimicrobial activity against the microorganisms listed in Table 4. Poor activity against these bacteria, despite strong inhibition of the enzyme in vitro, suggests that the compounds fail to penetrate bacterial cell membranes.

Conclusion

Structure-based design of a series of indazole-based SAH/MTA nucleosidase inhibitors led to the discovery of **20c**, a potent, low molecular weight inhibitor with nanomolar potency in an enzyme inhibition assay. In antimicrobial assays, this compound inhibits the growth of three important pathogenic species, showing MIC values less than 10 μM.

Experimental Section

General Chemistry Methods. Proton NMR spectra were run at 300 MHz on a Brüker Avance 300 spectrometer, and chemical shifts are reported in parts per million (δ) downfield from tetramethylsilane as internal standard. Atmospheric pressure ionization electrospray mass spectra and LCMS were recorded on an Agilent 1100 series LC/MSD-SL 1946D spectrometer equipped with an Agilent 100 series HPLC System. Silica gel 60 (230–400 mesh) from EM Science was used for column chromatography, and analytical or preparative thin-layer chromatography was conducted using EM Science Kieselgel 60 F_{254} plates. An Agilent 1100 Series HPLC with an Agilent Zorbax Eclipse XDB-C8 (4.6 X 150 mm) reversed phase column was used for analytical HPLC analyses. Preparative RP-HPLC was performed on a Gilson instrument with a MetaSil AQ 10 m C18 column. The elution buffer was an A/B gradient; A = H_2O–0.1% TFA, B = AcCN–0.1% TFA. For reactions performed under anhydrous conditions, glassware was either oven- or flame-dried, and the reaction was run under a positive pressure of nitrogen. Anhydrous solvents were used as purchased from commercial sources. Except where noted, reagents were purchased from commercial sources and used without further purification. The reported yields are the actual isolated yields of purified material and are not optimized.

3-Methyl-5-nitroindazole (4). 2-Chloro-5-nitroacetophenone (**2**) (1.00 g, 5 mmol) was dissolved in dry DMF (50 mL). To this solution was added anhydrous hydrazine (0.166 g, 165 μL, 5.2 mmol), and the mixture was heated at 110 °C for 16 h. The reaction mixture was then poured into saturated brine solution and extracted three times with diethyl ether. The combined extracts were then dried over MgSO$_4$, filtered, and concentrated. The resulting oil was purified by silica gel chromatography (20% ethyl acetate–hexane) providing (700 mg, 86%) of product **4**: ^{1}H NMR (CD$_3$OD) δ 8.74 (d, J = 0.02 Hz, 1 H), 8.24 (dd, J = 0.02, 0.1 Hz, 1 H), 7.57 (d, J = 0.1 Hz, 1 H), 2.62 (s, 3 H); LCMS (API-ES) m/z 176.0 [M − H].

5-Dimethylamino-naphthalene-1-sulfonic acid (1H-indazol-5-yl)-amide (9a) representative procedure for 9b–9h. To a solution of 1H-indazol-5-ylamine (**5**) (133 mg, 1.0 mmol) in dry pyridine (4 mL) was added dansyl chloride (297 mg, 1.1 mmol) portionwise with stirring at ambient temperature. The reaction mixture was allowed to stir for 2 h; after which time LCMS indicated complete consumption of starting aniline. The pyridine was removed in vacuo, and the residue

Table 3. Trisubstituted Indzole Inhibitors of SAH/MTA Nucleosidase: 5-Biarylsulfonamides

20a-p
21a-f
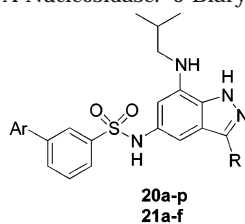
Compound	R	Ar	K_i (μM)	Compound	R	Ar	K_i (μM)
20a	Cl		0.0034	**20j**	Cl		0.0110
20b	Cl		0.0125	**21c**	Me		0.02
20c	Cl		0.0016	**20k**	Cl		0.0146
20d	Cl		0.0081	**20l**	Cl		0.013
20e	Cl		0.0108	**20m**	Cl		0.017
20f	Cl		0.036	**20n**	Cl		0.036
21a	Me		0.191	**21d**	Me		0.1
20g	Cl		0.0285	**20o**	Cl		0.094
20h	Cl		0.052	**21e**	Me		0.498
21b	Me		0.24	**20p**	Cl		0.025
20i	Cl		0.0039	**21f**	Me		0.125

was purified by RPHPLC (AcCN/H$_2$O, 1.0% TFA) to afford **9a** as a tan solid. ^{1}H NMR (DMSO-d_6) δ 13.30 (s, 1H), 10.63 (s, 1H), 8.45 (d, 1H), 8.05 (d, 1H), 7.88 (s, 1H), 7.55 (t, 1H), 7.35 (t, 1H), 7.28 (m, 2H), 7.25 (t, 2H), 6.94 (m, 1H), 2.87 (s, 6H); LCMS *m/z* 368.9, 367.0 [M + H$^+$]; 365.0, 366.0 [M + H$^-$].

5-Dimethylamino-naphthalene-1-sulfonic acid (1H-Indazol-6-yl)-amide (9b). ^{1}H NMR (DMSO-d_6) δ 13.40 (s, 1H), 11.03 (s, 1H), 8.48 (d, 1H), 8.38 (d, 1H), 8.18 (d, 1H), 7.92 (s, 1H), 7.58 (t, 1H), 7.45 (m, 2H), 7.25 (m, 2H), 6.68 (m, 1H), 2.86 (s, 6H); LCMS *m/z* 368.9, 367.0 [M + H$^+$]; 365.0, 367.0 [M + H$^-$].

5-Dimethylamino-naphthalene-1-sulfonic acid (3-chloro-1H-indazol-5-yl)-amide (9c). ^{1}H NMR (DMSO-d_6) δ 13.39 (s, 1H), 10.82 (s, 1H), 8.60 (m, 2H), 8.32 (m, 1H), 7.81−7.73 (m, 2H), 7.55 (m, 1H), 7.42 (m, 1H), 7.34 (m, 2H), 2.98 (s, 6H); LCMS *m/z* 380.9, 383.0 [M + H$^+$]; 379.1, 381.0 [M + H$^-$].
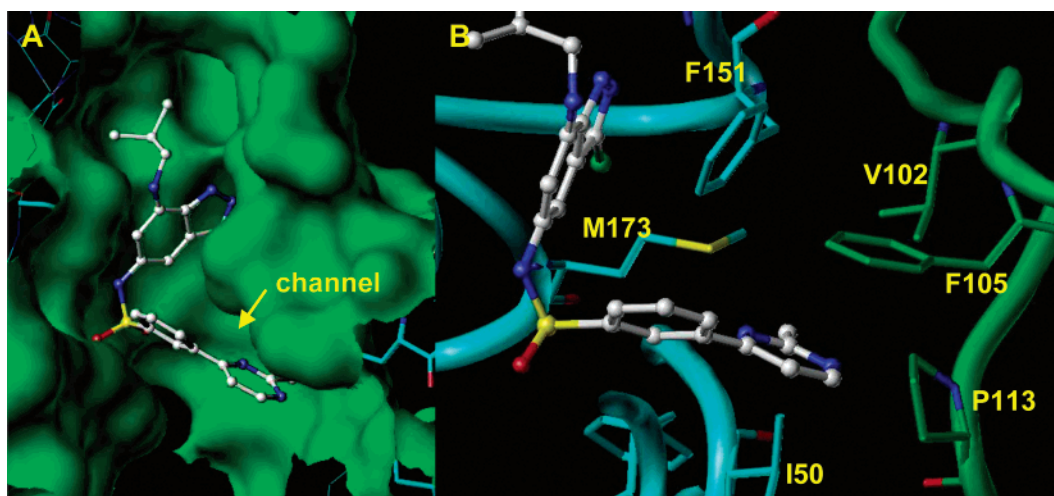
Figure 6. (A) Cocrystal structure of inhibitor **20f** ($K_i = 0.036$ μM) bound to SAH/MTA nucleosidase (solvent-accessible surface of the active site illustrated in green). (B) Ribbon diagram of the active site channel located at the dimer interface that accommodates the biarene portion of **20f**. The channel is comprised of residues I50, F151, and M173 from one monomer (cyan) and V102, F105, and P113 (green).

Table 4. Minimum Inhibitory Concentrations (MIC) for Select Indazole MTA Nucleosidase Inhibitors

compound	K_i (μM)	MIC (μM)		
		N. meningitidis	*S. pneumoniae*	*S. pyogenes*
18a	0.76	5	5	7.5
18b	0.5	5	-	>20
20a	0.0034	1.875	3.75	3.75
20b	0.0125	2.5	2.5	1.25
20c	0.0016	1.875	7.5	7.5
20h	0.052	10	-	>20
20i	0.0039	7.5	7.5	7.5
21c	0.02	20	-	>20
20l	0.013	5	-	>20
21d	0.1	20	-	>20
20o	0.094	2.5	-	>20

5-Dimethylamino-naphthalene-1-sulfonic Acid (3-methyl-1H-indazol-5-yl)-amide (9d). ^{1}H NMR (DMSO-d_6) δ 12.54 (s, 1H), 10.36 (s, 1H), 8.40 (m, 2H), 8.07 (m, 1H), 7.62−7.52 (m, 2H), 7.24 (m, 3H), 6.93 (m, 1H), 2.80 (s, 6H), 2.32 (s, 3H); LCMS m/z 380.9, 383.0 [M + H$^+$]; 379.1, 381.0 [M + H$^−$].

4-Chloro-N-(1H-indazol-5-yl)-benzenesulfonamide (9e). ^{1}H NMR (DMSO-d_6) δ 13.20 (s, 1H), 11.42 (s, 1H), 8.18 (s, 1H), 7.84, 7.75, (AA′,BB′, 2 × 2H), 7.60 (m, 2H), 7.23 (m, 1H); LCMS m/z 309.9, 307.0 [M + H$^+$]; 307.0, 305.0 [M + H$^−$].

4-Chloro-N-(1H-indazol-6-yl)-benzenesulfonamide (9f). ^{1}H NMR (DMSO-d_6) δ 12.89 (s, 1H), 10.48 (s, 1H), 7.96 (s, 1H), 7.74, 7.63, (AA′,BB′, 2 × 2H), 7.25 (s, 1H), 6.88 (m, 1H); LCMS m/z 309.9, 307.0 [M + H$^+$]; 307.0, 305.0 [M + H$^−$].

4-Chloro-N-(3-methyl-1H-indazol-5-yl)-benzenesulfonamide (9h). ^{1}H NMR (DMSO-d_6) δ 7.95−7.82 (m, 4H), 7.54 (s, 1H), 7.41 (d, $J = 8.7$ Hz, 1H), 7.15 (d, $J = 8.7$ Hz, 1H), 2.61 (s, 3H); LCMS m/z 322.7 [M + H$^+$]; 320.8 [M + H$^−$].

3-Methyl-5,7-dinitro-1H-indazole (11). 3-Methyl-5-nitroindazole (4) (2.36 g, 13 mmol) was dissolved in concentrated H$_2$SO$_4$ (75 mL) and cooled to 0° C. To this solution was added concentrated HNO$_3$ (2.70 mL, 53 mmol) and the reaction was stirred for 3 h while warming to room temperature. The crude solution was poured onto crushed ice (100 g), and the resulting solid was collected by vacuum filtration and dried over P$_2$O$_5$. The product **11** was isolated (3.75 g, 94%) as the sulfuric acid salt: ^{1}H NMR (DMSO-d_6) δ 9.27 (d, $J = 1.8$ Hz, 1 H), 8.94 (d, $J = 1.8$ Hz, 1 H), 2.67 (s, 3 H).

3-Chloro-5-nitro-7-amino-1(2)H-indazole (12). A solution of 3-chloro-5,7-dinitro-1(2)H-indazole (10) (2.0 g, 8.2 mmol) in EtOH (100 mL) was treated with 20% aqueous (NH$_4$)$_2$S (15 mL, 44.0 mmol) and the mixture was heated at 80 °C for 0.5 h. The solution was filtered, concentrated to one-third volume, and then poured into brine and extracted with EtOAc (3×).

The combined extracts were dried over MgSO$_4$, concentrated, and the crude product was purified by flash column chromatography (20% EtOAc−hexanes) to afford (1.5 g, 86%) of **12** as an orange solid: mp: 264−266 °C; ^{1}H NMR (DMSO-d_6) δ 13.51 (s, H), 7.79 (d, $J = 2.0$ Hz, 2H), 7.41 (d, $J = 2.0$ Hz, 2H), 6.16 (s, 2H); LCMS (API-ES) m/z 212.9, 214.9 [M + H$^+$]; 210.9, 222.9 [M + H$^−$].

7-Amino-5-nitroindazole (13). According to the procedure for compound **12** above, 5,7-dinitroindazole (**11**) (1.50 g, 6.8 mmol) and aq S(NH$_4$)$_2$ (2.93 M, 9.2 mL, 27 mmol) provided **13** (0.50 g, 61% yield) as a pale brown solid after silica gel chromatography (50% EtOAc−hexanes): ^{1}H NMR (DMSO-d_6) δ 12.76 (s, 1 H), 7.95 (d, $J = 0.02$ Hz, 1 H), 7.28 (d, $J = 0.02$ Hz, 1 H,), 5.90 (s, 2 H), 2.50 (s, 3 H); MS (API-ES) m/z 191 [M − H].

N-[3-Chloro-5-nitro-1H-indazol-7-yl]-acetamide (14a). To a solution of 3-chloro-5-nitro-7-amino-1(2)H-indazole (**12**) (500 mg, 2.3 mmol) in glacial AcOH (10 mL) was added Ac$_2$O (287 mg, 2.8 mmol). The reaction mixture was heated at 80 °C with stirring for 2 h. After cooling of the sample, the mixture was quenched (H$_2$O) and extracted with EtOAc (3 × 50 mL). The combined organic extracts were washed with NaHCO$_3$ and brine and dried (MgSO$_4$). Purification by silica gel chromatography (20% EtOAc−hexane) provided **14a** (380 mg, 63%) as a tan solid: mp: 186−188 °C; ^{1}H NMR (DMSO-d_6) δ 13.47 (s, H), 10.24 (s, H), 8.37 (d, $J = 2.0$ Hz, 1H), 8.36 (d, $J = 2.0$ Hz, 1H), 2.20 (s, 3H); LCMS m/z 254.9, 256.9 [M + H$^+$]; 254.9, 252.9 [M + H$^−$].

3-Chloro-5-nitro-7-isobutylamino-1(2)H-indazole (14b). 3-Chloro-5-nitro-7-amino-1(2)H-indazole (**12**) (200 mg, 0.94 mmol) in AcCN (10 mL) was allowed to react with isovaleraldehyde (80 mg, 1.1 mmol) and NaBH(OAc)$_3$ (0.3 g, 1.4 mmol) at ambient temperature for 18 h. Evaporation to dryness and purification by silica gel chromatography (20% EtOAc−hexane) afforded **14b** (180 mg, 72%) as an orange-red solid: mp: 178−180 °C; ^{1}H NMR (DMSO-d_6) δ 13.32 (s, H), 7.64 (d, $J = 2.0$ Hz, 1H), 6.96 (d, $J = 2.0$ Hz, 1H), 5.99 (m, 1H), 2.98 (m, 2H), 1.88 (m, 1H), 0.91 (m, 6H); LCMS m/z 269.0, 271.0 [M + H$^+$]; 267.0, 269.0 [M + H$^−$].

Intermediates 14c−14j. Synthesized according to the general procedure above using 3-chloro-5-nitro-7-amino-1(2)-H-indazole (**12**) (1 equiv), the appropriate aldehyde (1.2 equiv) and NaBH(OAc)$_3$ (1.5 equiv) in AcCN. The products thusly derived were used directly without purification.

3-Chloro-5-amino-7-isobutylamino-1(2)H-indazole (16b). A mixture of 3-chloro-5-nitro-7-isobutylamino-1(2)H indazole (**14b**) (200 mg, 0.94 mmol), SnCl$_2$·H$_2$O (1.0 g, 4.7 mmol) in EtOH (10 mL) was heated at reflux for 18 h. The mixture was cooled to room temperature, diluted with saturated aq NaHCO$_3$, and extracted with EtOAc. The combined organic extracts

were dried (MgSO$_4$) and concentrated, and the product was purified by silica gel chromatography (20% EtOAc−hexane) affording **16b** (180 mg, 72%) as an orange solid: mp: 143−145 °C; ^{1}H NMR (DMSO-d_6) δ 13.11 (s, 1H), 10.01 (bs, 2H), 6.59 (d, J = 2.0 Hz, 1H), 6.16 (d, J = 2.0 Hz, 1H), 2.94 (m, 2H), 1.88 (m, 1H), 1.05 (s, 3H), 1.03 (s, 3H); LCMS m/z 238.9, 240.9 [M + H$^+$]; 236.9, 238.9 [M + H$^-$].

Intermediates 16a, 16c−16j. Synthesized according to the procedure above for **16b** using crude **14a**, **14c−14j** (1 equiv), SnCl$_2$·H$_2$O (4.7 equiv) and EtOH. Extractive workup yielded the crude 5-aminoindazoles which were used without further purification.

***N*-[3-Chloro-5-(4-chloro-benzenesulfonylamino)-1H-in-dazol-7-yl]-acetamide (18a).** 3-Chloro-5-amino-7-acetamide-1(2)*H*-indazole (**16a**) (20 mg, 0.09 mmol) dissolved in dry pyridine (5 mL) was allowed to react with 4-chlorobenzene sulfonyl chloride (23 mg, 0.1 mmol) at ambient temperature for 16 h. The mixture was concentrated to dryness, recovered in EtOAc, and washed with saturated aq. NaHCO$_3$ and brine. Removal of solvent and purification by RP-HPLC (AcCN/H$_2$O, 1.0% TFA) afforded **18a** (26 mg, 75%) as a tan solid: ^{1}H NMR (DMSO-d_6) δ 12.73 (s, 1H), 10.06 (s, 1H), 7.73, 7.63, (AA′,BB′, 2 × 2H), 6.54 (d, J = 2.0 Hz, 1H), 6.12 (d, J = 2.0 Hz,1H), 5.82 (m, 1H), 2.11 (s, 3H); LCMS m/z 398.9, 400.9 [M + H$^+$]; 396.8, 398.9 [M + H$^-$].

4-Chloro-*N*-(3-chloro-7-isobutylamino-1H-indazol-5-yl)-benzenesulfonamide (18b). Prepared from **16b** according to the general procedure above: ^{1}H NMR (DMSO-d_6) δ 7.79, 7.68 (AA′,BB′, 2 × 2H) 6.58 (d, J = 2.0 Hz, 1H), 6.14 (d, J = 2.0 Hz, 1H), 2.92 (m, 2H), 1.86 (m, 1H), 1.03 (s, 3H), 1.01 (s, 3H); LCMS m/z 412.9, 414.9 [M + H$^+$]; 410.9, 412.9 [M + H$^-$].

4-Chloro-N-[3-chloro-7-(cyclopropylmethyl-amino)-1H-indazol-5-yl]-benzenesulfonamide (18c). Prepared from **16c** according to the general procedure above: ^{1}H NMR (DMSO-d_6) δ 12.81 (s, 1H), 10.03 (s, 1H), 7.71, 7.61 (AA′,BB′, 2 × 2H),6.51 (d, J = 2.0 Hz, 1H), 6.14 (d, J = 2.0 Hz, 1H), 5.82 (m, 1H), 2.90 (d, 2H), 1.04 (m, 1H), 0.53 (m, 2H), 0.26 (m, 2H); LCMS m/z 410.9, 412.9 [M + H$^+$]; 408.9, 410.9 [M + H$^-$].

4-Chloro-*N*-[3-chloro-7-(2,2-dimethyl-propylamino)-1H-indazol-5-yl]-benzenesulfonamide (18d). Prepared from **16d** according to the general procedure above: ^{1}H NMR (DMSO-d_6) δ 12.60 (s, 1H), 9.99 (s, 1H), 7.70, 7.58 (AA′,BB′, 2 × 2H), 6.51 (d, J = 2.0 Hz, 1H), 6.14 (d, J = 2.0 Hz, 1H), 5.82 (m, 1H), 2.82 (s, 2H), 0.95 (s, 9H); LCMS m/z 427.0, 428.9 [M + H$^+$]; 424.9, 427.0 [M + H$^-$].

4-Chloro-*N*-(3-chloro-7-(ethylamino)-1H-indazol-5-yl)-benzenesulfonamide (18e). Prepared from **16e** according to the general procedure above: ^{1}H NMR (DMSO-d_6) δ 12.85 (s, 1H), 10.06 (s, 1H), 7.71, 7.61 (AA′,BB′, 2 × 2H), 6.49 (d, J = 2.0 Hz, 1H), 6.15 (d, J = 2.0 Hz, 1H), 5.65 (m, 1H), 3.07 (m, 2H),1.22 (t, 3H); LCMS m/z 384.9, 386.9 [M + H$^+$]; 382.9, 384.9 [M + H$^-$].

4-Chloro-*N*-[3-chloro-7-(3-methyl-butylamino)-1H-in-dazol-5-yl]-benzenesulfon amide (18f). Prepared from **16f** according to the general procedure above: ^{1}H NMR (DMSO-d_6) δ 12.82 (s, 1H), 10.10 (s, 1H), 7.76, 7.67 (AA′,BB′, 2 × 2H),0.98 (m, 6H), 1.52 (m, 2H), 1.76 (m, 1H), 3.10 (m, 2H), 5.82 (m, 1H), 6.17 (d, J = 2.0 Hz, 1H), 6.56 (d, J = 2.0 Hz, 1H); LCMS m/z 427.0, 428.9 [M + H$^+$]; 424.9, 426.9 [M + H$^-$].

4-Chloro-*N*-[3-chloro-7-(3,3-dimethyl-butylamino)-1H-indazol-5-yl]-benzenesulfonamide (18 g). Prepared from **16g** according to the general procedure above: ^{1}H NMR (DMSO-d_6) δ 12.73 (s, 1H), 10.06 (s, 1H), 7.73, 7.63 (AA′,BB′, 2 × 2H), 6.54 (d, J = 2.0 Hz, 1H), 6.12 (d, J = 2.0 Hz, 1H), 5.82 (m, 1H), 3.05 (m, 2H), 1.50 (m, 2H), 0.98 (s, 9H); LCMS m/z 440.9, 443.0 [M + H$^+$]; 438.9, 440.9 [M + H$^-$].

4-Chloro-*N*-[3-chloro-7-(3-methyl-but-2-enylamino)-1H-indazol-5-yl]-benzenesulfonamide (18h). Prepared from **16h** according to the general procedure above: ^{1}H NMR (DMSO-d_6) δ 12.70 (s, 1 H), 10.07 (s, 1 H), 7.71 (m, 2 H), 7.61 (m, 2 H), 6.50 (s, 1 H), 6.15 (s, 1 H), 5.27 (m, 1H), 3.63 (d, J = 6.4, 2 H), 1.74 (s, 3 H), 1.70 (s, 3 H); LCMS (API-ES) m/z 425.0 and 427.0 [M + H$^+$], 423.0 and 425.0 [M − H$^-$].

***N*-(7-Benzylamino-3-chloro-1H-indazol-5-yl)-4-chloro-benzenesulfonamide (18i).** Prepared from **16i** according to the general procedure above: ^{1}H NMR (DMSO-d_6) δ 12.90 (s, 1H), 10.18 (s, 1H), 7.65 (m, 4H), 7.48 (m, 5H), 6.61 (d, J = 2.0 Hz, 1H), 6.36 (d, J = 2.0 Hz, 1H), 4.43 (s, 2H); LCMS m/z 445.9, 447.9 [M + H$^+$]; 443.9, 445.9 [M + H$^-$].

4-Chloro-*N*-(3-chloro-7-phenethylamino-1H-indazol-5-yl)-benzenesulfonamide (18j). Prepared from **16j** according to the general procedure above: ^{1}H NMR (DMSO-d_6) δ 12.63 (s, 1H), 9.96 (s, 1H), 7.13−7.62 (m, 9H), 6.42 (d, J = 2.0 Hz, 1H), 6.13 (d, J = 2.0 Hz, 1H), 3.18 (m, 2H), 2.72 (m, 2H); LCMS m/z 460.8, 462.8 [M + H$^+$]; 458.9, 460.8 [M + H$^-$].

3-Bromo-*N*-(3-chloro-7-isobutylamino-1H-indazol-5-yl)-benzenesulfonamide (18k). Prepared from **16b** accord-ing to the general procedure above: mp; 243−245 °C; ^{1}H NMR (DMSO-d_6) δ 12.84 (s, 1H), 10.11 (s, 1H), 7.88 (m, 2H), 7.76 (m, 1H), 7.74 (m, 1H), 6.56 (d, J = 2.0 Hz, 1H), 6.16 (d, J = 2.0 Hz, 1H), 5.80 (m, 1H), 2.91 (m, 2H), 1.88 (m, 1H), 1.02 (s, 3H),1.01 (s, 3H); LCMS m/z 457.0, calcd mass 457.78 (C$_{17}$H$_{18}$-BrClN$_4$O$_2$S).

3-Bromo-*N*-(7-isobutylamino-3-methyl-1H-indazol-5-yl)-benzenesulfonamide (19a). To a solution of *N*-7-isobutyl-3-methyl-1H-indazole-5,7-diamine hydrochloride (**17**) (367 mg, 1.44 mmol) in dry pyridine (5 mL) was added 3-bromobenze-nesulfonyl chloride (370 mg, 1.44 mmol) portionwise with stirring at ambient temperature. The reaction mixture was allowed to stir for 2 h; after which time LCMS indicates complete consumption of starting aniline. The pyridine was removed in vacuo, and the residue was dissolved in EtOAc (30 mL) and washed with 1% aq HCl and brine and dried over anhydrous Na$_2$SO$_4$. Removal of solvent and purification by flash chromatography (40−60% EtOAc/hexanes) provided **19a** as a tan solid (460 mg, 73%): ^{1}H NMR (DMSO-d_6) δ 12.14 (s, 1 H), 9.80 (s, 1 H), 7.85 (s, 1 H), 7.80 (d, J = 7.1 Hz, 1 H), 7.77 (d, J = 7.1 Hz, 1 H), 7.46 (t, J = 8.0 Hz, 1 H), 6.56 (s, 1 H), 5.92 (s, 1 H), 5.56 (m, 1H), 2.80 (t, J = 6.1 Hz, 2 H), 2.31 (s, 3 H), 1.70 (m, 1 H), 0.93 (s, 3 H), 0.91 (s, 3 H); ^{13}C NMR (75 MHz, DMSO-d_6) δ 179.3, 165.4, 165.0, 156.7, 147.4, 132.3, 130.7, 129.1, 129.0, 108.0, 104.7, 102.5, 98.0, 54.3, 43.0, 30.3, 27.5; LCMS (API-ES) m/z 436.9, 439.0 [M + H$^+$]; 434.9, 436.9 [M − H$^-$].

General Procedure for the Preparation of Biaryl Sulfonamides 20 and 21 via Pd-Mediated Cross Cou-pling. A mixture of 3-bromobenzenesulfonamide derivative (1 equiv), Pd(PPh$_3$)$_4$ (3 mol %), aryl boronic acid or ester (1.5 equiv), 2 M aq Na$_2$CO$_3$ (3 equiv) in DME (to 0.5 M sulfonamide) is heated at 85 °C under an inert atmosphere for 5 h or until HPLC or TLC analysis indicates complete reaction. The mixture is then concentrated in vacuo, dissolved in EtOAc (20 mL), and washed with H$_2$O (2 × 5 mL) and brine (1 × 5 mL) and dried over anhydrous Na$_2$SO$_4$. Removal of solvent affords the crude product that is purified by RP-HPLC.

3′-Chloro-4′-fluoro-biphenyl-3-sulfonic Acid (3-chloro-7-isobutylamino-1H-indazol-5-yl)-amide (20a). Synthe-sized according to the general procedure using **18k** (50 mg, 0.1 mmol), 3-chloro-4-fluorophenylboronic acid (28 mg, 0.16 mmol) and Pd(PPh$_3$)$_4$ (2.0 mg). The crude product was purified by RP-HPLC (AcCN/H$_2$O, 1.0% TFA), affording **20a** (44 mg, 80%) as a tan solid: ^{1}H NMR (DMSO-d_6) δ 12.78 (s, 1H), 9.92 (s, 1H), 8.01 (s, 1H), 7.54−7.96 (m, 8H), 6.58 (d, J = 2.0 Hz, 1H), 6.16 (d, J = 2.0 Hz, 1H), 5.71 (m, 1H), 2.72 (d, 2H), 1.77 (m, 1H), 0.89 (s, 3H), 0.87 (s, 3H); LCMS m/z 506.9, 508.9 [M + H$^+$]; 504.8, 506.9 [M + H$^-$].

4′-Chloro-biphenyl-3-sulfonic Acid (3-chloro-7-isobu-tylamino-1H-indazol-5-yl)amide (20b). Derived from **16b** according to the general sulfonamide coupling conditions described for **18a**: ^{1}H NMR (DMSO-d_6) δ 12.64 (s, 1H), 10.11 (s, 1H), 7.93 (s, 1H), 7.45−7.83 (m, 8H), 6.58 (d, J = 2.0 Hz, 1H), 6.17 (d, J = 2.0 Hz, 1H), 2.72 (d, 2H), 1.78 (m, 1H), 0.89 (s, 3H), 0.87 (s, 3H); LCMS m/z 488.9, 490.9 [M + H$^+$]; 486.8, 488.9 [M + H$^-$].

3′,4′-Dichloro-biphenyl-3-sulfonic Acid (3-chloro-7-isobutylamino-1H-indazol-5-yl)-amide (20c). Prepared ac-cording to the general sulfonamide coupling procedure. ^{1}H NMR (DMSO-d_6) δ 12.74 (s, 1 H), 9.93 (s, 1 H), 8.03 (m, 1 H),

7.94 (m, 1 H), 7.83 (m, 1 H), 7.74 (m, 2 H), 7.61 (m, 2 H), 6.55 (s, 1 H), 6.13 (s, 1 H), 5.70 (m, 1H), 2.78 (d, $J = 6.6$ Hz, 2 H), 1.73 (m, 1 H), 0.84 (d, $J = 6.8$ Hz, 6 H); LCMS (API-ES) m/z 523.0, 525.0 [M + H$^+$], 521.0, 523.0 [M − H$^-$].

3′,4′-Difluoro-biphenyl-3-sulfonic Acid (3-Chloro-7-isobutylamino-1H-indazol-5-yl)-amide (20d). Prepared according to the general Pd-mediated cross coupling procedure: ^{1}H NMR (DMSO-d_6) δ 12.74 (s, 1 H), 9.93 (s, 1 H), 8.01 (m, 1 H), 7.90 (m, 1 H), 7.74−7.43 (m, 5 H), 6.55 (s, 1 H), 6.14 (s, 1 H), 5.69 (m, 1H), 2.79 (d, $J = 6.6$ Hz, 2 H), 1.84 (m, 1 H), 0.94 (d, $J = 6.6$ Hz, 6 H); LCMS (API-ES) m/z 491.0 [M + H$^+$], 489.0 [M − H$^-$].

***N*-(3-Chloro-7-isobutylamino-1H-indazol-5-yl)-3-quinolin-3-yl-benzenesulfonamide (20e).** Prepared according to the general Pd-mediated cross coupling procedure: ^{1}H NMR (DMSO-d_6) δ 12.85 (s, 1H), 10.01 (s, 1H), 9.26 (s, 1H), 9.25 (s, 1H), 8.63 (s, 1H), 7.75−8.25 (m, 8H), 6.67 (d, $J = 2.0$ Hz, 1H), 6.25 (d, $J = 2.0$ Hz, 1H), 5.72 (m, 1H), 2.86 (d, 2H), 1.80 (m, 1H), 0.88 (s, 3H), 0.86 (s, 3H); LCMS m/z 506.0, 508.0 [M + H$^+$]; 503.9, 505.9 [M + H$^-$].

***N*-(3-Chloro-7-isobutylamino-1H-indazol-5-yl)-3-(2-methyl-pyrimidin-4-yl)-benzenesulfonamide (20f).** Prepared according to the general sulfonamide coupling procedure: ^{1}H NMR (DMSO-d_6) δ 12.79 (s, 1H), 10.13 (s, 1H), 8.87 (d, 1H), 8.68 (s, 1H), 8.35 (d, 1H), 7.94 (m, 2H), 7.75 (m, 2H), 6.61 (d, $J = 2.0$ Hz, 1H), 6.18 (d, $J = 2.0$ Hz, 1H), 3.53 (s, 3H), 2.86 (m, 2H), 1.89 (m, 1H), 0.92 (s, 3H), 0.89 (s, 3H); LCMS m/z 470.9, 473.0 [M + H$^+$]; 469.0, 470.9 [M + H$^-$].

***N*-(3-Chloro-7-isobutylamino-1H-indazol-5-yl)-3-(2-methyl-pyridin-4-yl)-benzenesulfonamide (20 g).** Prepared according to the general Pd-mediated cross coupling procedure: ^{1}H NMR (DMSO-d_6) δ 12.76 (s, 1 H), 9.99 (s, 1 H), 8.66 (m, 1 H), 8.12 (m, 1 H), 8.07 (m, 1 H), 7.85 (m, 1 H), 7.70 (m, 3 H), 6.67 (s, 1 H), 6.14 (s, 1 H), 5.70 (m, 1H), 2.80 (d, $J = 6.6$, 2 H), 2.60 (s, 3 H), 1.75 (m, 1 H), 0.86 (d, $J = 6.3$ Hz, 6 H); LCMS (API-ES) m/z 470.0 [M + H$^+$], 468.0 [M − H$^-$].

***N*-(3-Chloro-7-isobutylamino-1H-indazol-5-yl)-3-pyridin-4-yl-benzenesulfonamide (20h).** Prepared according to the general Pd-mediated cross coupling procedure: ^{1}H NMR (DMSO-d_6) δ 12.76 (s, 1 H), 10.03 (s, 1 H), 8.80 (d, $J = 5.3$ Hz, 1 H), 8.19 (s, 1 H), 8.09 (d, $J = 7.8$ Hz, 1 H), 7.85 (m, 1 H), 7.88 (d, $J = 6.0$ Hz, 2 H), 7.83 (d, $J = 7.8$ Hz, 1 H), 7.71 (t, $J = 7.8$ Hz, 1 H), 6.54 (s, 1 H), 6.14 (s, 1 H), 5.71 (m, 1H), 2.80 (d, $J = 6.7$, 2 H), 1.74 (m, 1 H), 0.85 (d, $J = 6.6$ Hz, 6 H); LCMS (API-ES) m/z 456.0 [M + H$^+$], 454.0 [M − H$^-$].

4′-Chloro-3′-methyl-biphenyl-3-sulfonic Acid (3-chloro-7-isobutylamino-1H-indazol-5-yl)-amide (20i). Prepared according to the general Pd-mediated cross coupling procedure: ^{1}H NMR (DMSO-d_6) δ 12.75 (s, 1H), 9.94 (s, 1H), 7.94 (s, 1H), 7.40−7.80 (m, 7H), 6.55 (d, $J = 2.0$ Hz, 1H), 6.13 (d, $J = 2.0$ Hz, 1H), 5.72 (m, 1H), 2.80 (d, 2H), 2.37 (s, 3H), 1.81 (m, 1H), 0.86 (s, 3H), 0.84 (s, 3H); LCMS m/z 502.9, 504.9 [M + H$^+$]; 500.9, 502.9 [M + H$^-$].

3′-Trifluoromethyl-biphenyl-3-sulfonic Acid (3-chloro-7-isobutylamino-1H-indazol-5-yl)-amide (20j). Prepared according to the general Pd-mediated cross coupling procedure: ^{1}H NMR (DMSO-d_6) δ 12.73 (s, 1H), 9.96 (s, 1H), 8.07 (s, 1H), 7.60−7.80 (m, 8H), 6.56 (d, 1H, $J = 2.0$ Hz), 6.12 (d, 1H, $J = 2.0$ Hz), 5.69 (m, 1H), 2.77 (d, 2H), 1.72 (m, 1H), 0.90 (s, 3H), 0.88 (s, 3H); LCMS m/z 523.0, 524.9 [M + H$^+$]; 520.8, 522.8 [M + H$^-$].

4′-Fluoro-3′-methyl-biphenyl-3-sulfonic Acid (3-chloro-7-isobutylamino-1H-indazol-5-yl)-amide (20k). Prepared according to the general Pd-mediated cross coupling procedure: ^{1}H NMR (DMSO-d_6) δ 12.75 (s, 1H), 9.92 (s, 1H), 7.99 (s, 1H), 7.51−7.93 (m, 7H), 6.55 (d, $J = 2.0$ Hz, 1H), 6.13 (d, $J = 2.0$ Hz, 1H), 5.71 (m, 1H), 3.44 (s, 3H), 2.78 (d, 2H), 1.74 (m, 1H), 0.85 (s, 3H), 0.83 (s, 3H); LCMS m/z 487.0, 489.0 [M + H$^+$]; 484.9, 486.9 [M + H$^-$].

4′-Trifluoromethyl-biphenyl-3-sulfonic Acid (3-chloro-7-isobutylamino-1H-indazol-5-yl)-amide (20l). Prepared according to the general sulfonamide coupling procedure: ^{1}H NMR (DMSO-d_6) δ 12.76 (s, 1 H), 10.00 (s, 1 H), 8.07 (m, 1 H), 7.96 (m, 1 H), 7.83 (m, 4 H), 7.75 (m, 1 H), 7.64 (m, 1 H), 6.55 (s, 1 H), 6.14 (s, 1 H), 5.70 (m, 1H), 2.78 (d, $J = 5.7$ Hz, 2 H),

1.73 (m, 1 H), 0.83 (d, $J = 6.6$ Hz, 6 H); LCMS (API-ES) m/z 523.1 [M + H$^+$], 521.1 [M − H$^-$].

3′-Methylsulfanyl-biphenyl-3-sulfonic Acid (3-chloro-7-isobutylamino-1H-indazol-5-yl)-amide (20m). Prepared according to the general Pd-mediated cross coupling procedure: ^{1}H NMR (DMSO-d_6) δ 12.87 (s, 1H), 9.99 (s, 1H), 8.02 (s, 1H), 7.23−7.79 (m, 8H), 6.59 (d, $J = 2.0$ Hz, 1H), 6.18 (d, $J = 2.0$ Hz, 1H), 5.70 (m, 1H), 3.71 (s, 3H), 2.74 (d, 2H), 1.79 (m, 1H), 0.90 (s, 3H), 0.88 (s, 3H); LCMS m/z 500.9, 503.0 [M + H$^+$]; 499.0, 500.9 [M + H$^-$].

3′-Methyl-biphenyl-3-sulfonic Acid (3-chloro-7-isobutylamino-1H-indazol-5-yl)-amide (20n). Prepared according to the general Pd-mediated cross coupling procedure: ^{1}H NMR (DMSO-d_6) δ 12.81 (s, 1H), 9.90 (s, 1H), 7.86 (s, 1H), 7.17−7.80 (m, 8H), 6.60 (d, $J = 2.0$ Hz, 1H), 6.19 (d, $J = 2.0$ Hz, 1H), 5.70 (m, 1H), 2.74 (d, 2H), 2.28 (s, 3H), 1.81 (m, 1H), 0.90 (s, 3H), 0.88 (s, 3H); LCMS m/z 469.0, 471.0 [M + H$^+$]; 467.0, 469.0 [M + H$^-$].

Biphenyl-3-sulfonic Acid (3-chloro-7-isobutylamino-1H-indazol-5-yl)-amide (20o). Prepared according to the general sulfonamide coupling procedure: ^{1}H NMR (DMSO-d_6) δ 12.80 (s, 1H), 10.04 (s, 1H), 7.93 (s, 1H), 7.90 (d, 1H), 7.62 (d, 1H), 7.52 (m, 3H), 7.38 (m, 3H), 6.50 (d, $J = 2.0$ Hz, 1H), 6.20 (d, $J = 2.0$ Hz, 1H), 2.84 (m, 2H), 1.80 (m, 1H), 0.91 (s, 3H), 0.88 (s, 3H); LCMS m/z 455.0, 457.0 [M + H$^+$]; 452.9, 454.9 [M + H$^-$].

3′-(2-Hydroxy-ethyl)-biphenyl-3-sulfonic Acid (3-chloro-7-isobutylamino-1H-indazol-5-yl)-amide (20p). Prepared according to the general Pd-mediated cross coupling procedure: ^{1}H NMR (DMSO-d_6) δ 12.74 (s, 1 H), 9.96 (s, 1 H), 7.97 (m, 1 H), 7.86 (m, 1 H), 7.68 (m, 1 H), 7.58 (m, 1 H), 7.39 (m, 3 H), 7.27 (m, 1 H), 6.56 (s, 1 H), 6.16 (s, 1 H), 5.67 (m, 1H), 3.63 (t, $J = 6.9$, 2 H) 2.78 (m, 4 H), 1.76 (m, 1 H), 0.87 (d, $J = 6.3$ Hz, 6 H); LCMS (API-ES) m/z 499.1 [M + H$^+$], 497.1 [M − H$^-$].

***N*-(7-Isobutylamino-3-methyl-1H-indazol-5-yl)-3-(2-methyl-pyrimidin-4-yl)-benzenesulfonamide (21a).** Prepared according to the general sulfonamide coupling procedure: ^{1}H NMR (DMSO-d_6) δ 9.77 (s, 1 H), 8.73 (d, $J = 5.3$ Hz, 1 H), 8.54 (s, 1 H), 8.30 (d, $J = 7.1$ Hz, 1H), 7.80 (d, $J = 5.4$ Hz, 1 H), 7.76 (d, $J = 7.9$ Hz, 1 H), 7.60 (t, $J = 7.8$ Hz, 1 H), 6.55 (s, 1 H), 5.89 (s, 1H), 2.65 (d, $J = 6.1$ Hz, 2 H), 2.61 (s, 3H), 2.24 (s, 3 H), 1.62 (m, 1 H), 0.75 (s, 3 H), 0.73 (s, 3 H); LCMS (API-ES) m/z 450.6, [M + H$^+$] 451.0.

***N*-(7-Isobutylamino-3-methyl-1H-indazol-5-yl)-3-pyridin-4-yl-benzenesulfonamide (21b).** Prepared according to the general Pd-mediated cross coupling procedure: ^{1}H NMR (300 MHz, DMSO-d_6) δ 9.72 (s, 1 H), 8.70 (d, $J = 5.4$ Hz, 2 H), 8.09 (s, 1 H), 8.05 (d, $J = 8.6$ Hz, 1H), 7.78 (d, $J = 5.5$ Hz, 2 H), 7.76 (d, $J = 7.9$ Hz, 1 H), 7.62 (t, $J = 7.8$ Hz, 1 H), 6.55 (s, 1 H), 5.90 (s, 1H), 2.67 (d, $J = 6.6$ Hz, 2 H), 2.24 (s, 3 H), 1.64 (m, 1 H), 0.78 (s, 3 H), 0.76 (s, 3 H); LCMS (API-ES) m/z 435.5, [M + H$^+$] 436.0.

3′-Trifluoromethyl-biphenyl-3-sulfonic Acid (7-isobutylamino-3-methyl-1H-indazol-5-yl)-amide (21c). Prepared according to the general Pd-mediated cross coupling procedure: ^{1}H NMR (300 MHz, DMSO-d_6) δ 9.74 (s, 1 H), 8.06 (s, 1 H), 7.75 (m, 7 H), 6.63 (s, 1 H), 5.95 (s, 1H), 2.70 (d, $J = 4.3$ Hz, 2 H), 2.31 (s, 3 H), 1.71 (m, 1 H), 0.79 (m, 6 H); LCMS (API-ES) m/z 503.0 [M + H$^+$]; 501.0 [M − H$^-$].

3′-Methyl-biphenyl-3-sulfonic Acid (7-isobutylamino-3-methyl-1H-indazol-5-yl)-amide (21d). Prepared according to the general Pd-mediated cross coupling procedure: ^{1}H NMR (DMSO-d_6) δ 9.69 (s, 1 H), 7.89 (s, 1 H), 7.64 (d, $J = 7.7$ Hz, 1 H), 7.33 (m, 4 H), 6.61 (s, 1 H), 5.98 (s, 1H), 2.70 (d, $J = 5.7$ Hz, 2 H), 2.31 (m, 6 H), 1.71 (m, 1 H), 0.82 (m, 6 H); LCMS (API-ES) m/z 449.0 [M + H$^+$]; 447.0 [M − H$^-$].

Biphenyl-3-sulfonic Acid (7-isobutylamino-3-methyl-1H-indazol-5-yl)-amide (21e). Prepared according to the general sulfonamide coupling procedure: ^{1}H NMR (DMSO-d_6) δ 9.72 (s, 1 H), 7.96 (s, 1 H), 7.85 (d, $J = 7.6$ Hz, 1 H), 7.65 (d, $J = 7.7$ Hz, 1 H), 7.56 (t, $J = 7.5$ Hz, 1 H), 7.42 (m, 5 H), 6.61 (s, 1 H), 6.00 (s, 1H), 2.74 (t, $J = 6.8$ Hz, 2 H), 2.30 (s, 3 H), 1.71 (m, 1 H), 0.83 (s, 3 H), 0.81 (s, 3 H); ^{13}C NMR (75 MHz, DMSO-d_6) δ 179.3, 165.4, 165.0, 156.7, 147.4, 132.3,

130.7, 129.1, 129.0, 108.0, 104.7, 102.5, 98.0, 54.3, 43.0, 30.3, 27.5; LCMS (API-ES) *m/z* 435.0 [M + H$^+$]; 433.0 [M − H$^-$].

3′-Ethyl-biphenyl-3-sulfonic Acid *N*-(7-Isobutylamino-3-methyl-1H-indazol-5-yl)-3-amide (21f). Prepared according to the general Pd-mediated cross coupling procedure: ^{1}H NMR (300 MHz, DMSO-*d*$_6$) δ 9.65 (s, 1 H), 7.85 (s, 1H), 7.80 (d, *J* = 7.8 Hz, 1 H), 7.59 (d, *J* = 7.8 Hz, 1H), 7.50(t, *J* = 7.8 Hz, 1 H), 7.30 (d, *J* = 5.5 Hz, 2 H), 7.24 (s, 1 H), 7.22 (m, 1 H), 6.56 (s, 1H), 5.93 (s, 1H), 2.68 (d, *J* = 6.7 Hz, 2 H), 2.55 (q, *J* = 7.5 Hz, 2H), 2.25 (s, 3 H), 1.65 (m, 1 H), 1.12 (t, *J* = 7.6 Hz, 3H), 0.77 (s, 3 H), 0.75 (s, 3 H); LCMS (API-ES) *m/z* 462.6, [M + H$^+$] 463.1.

Computational Chemistry Methods. Homology modeling for MTA nucleosidase utilized the published *E. coli* MTA nucleosidase sequence, the homology program COMPOSER (Tripos, Inc. St. Louis, MO), and the published crystal structures for human MTA phosphorylase (1CG6.pdb),[3] human PNP (1A9Q.pdb)[2], and *E. coli* PNP (1A69.pdb).[11] Protein and small molecule modeling visualization were accomplished with Sybyl v. 6.7 (Tripos, Inc., St. Louis, MO) and Macromodel v. 4.1 (Schrödinger, Inc., Portland, OR). Handling of the small molecule virtual library, calculations of Lipinski properties, conversion of the library to 3D structures, calculation of 2D fingerprints, diversity clusters and selection were accomplished by the Unity 4.2, CONCORD, and SELECTOR modules in the Tripos suite (Tripos, Inc., St. Louis, MO). The virtual library of commercially available compounds was comprised of the Available Chemical Directory (MDL, San Leandro, CA) and libraries from three other vendors. Protein-small molecule docking experiments were performed using FlexX. Conformational energies and solvation free energies were calculated using Spartan (Wavefunction, Inc., Irvine, CA).

Expression and Purification of SAH/MTA Nucleosidase. A C-terminally His-tagged, full-length *E. coli pfs* gene encoding 238 amino acids was generated by PCR, inserted into the pET 11a expression vector, and transformed into the *E. coli* strain BL21-Gold (DE3) pLysS for protein expression. Protein expression was induced in the transformed *E. coli* cells using IPTG in the presence of ampicillin. Cells were harvested by centrifugation at 4 °C and frozen before lysis. Cells were thawed at ambient temperatures and resuspended in ice-cold buffer A (25 mM Tris pH 8.5/ 5 mM DTT/ 5% v/v glycerol) with 20 mM NaCl and lysed by microfluidization using Microfluidics L-110 per manufacturers recommended protocol. Crude lysate was fractionated by centrifugation at 12000*g* for 30 min. The tagged SAH/MTA nucleosidase protein was purified from the supernatant fraction by IMAC. Eluted protein was dialyzed against 20 mM KH$_2$PO$_4$, pH 7.0/100 mM NaCl, concentrated to 15 mg/mL, and used for crystallization and enzymatic assays. Cloning, purification, and assay of pathogenic SAH/MTA nucleosidase proteins were performed similarly. All other clones had an N-terminal histidine tag.

Enzymatic Assays. Spectrophotometric SAH detection assays were performed in 96-well microtiter plates as follows; in a final volume of 200 *μ*L, 1.4 nM *E. coli* MTA nucleosidase was incubated for 30 min at room temperature with 25 *μ*M SAH and 50 *μ*M inhibitor in 50 mM Hepes pH 7.5/2.5% DMSO. The SAH/MTA nucleosidase reaction was terminated by the addition of 20 *μ*L of SAH hydrolase and adenosine deaminase mixture at final concentrations of 0.01 mg/mL SAH hydrolase; 4.1 *μ*g/mL adenosine deaminase and incubated for an additional 30 min. Color development was achieved by adding DTNB to 100 *μ*M, incubating for 10 min and then reading at A405. The absorbance level was proportional to the amount of SAH that did not get turned over during the SAH/MTA nucleosidase reaction.

Direct HPLC assays were performed in 96-well microtiter plates as follows: in a final volume of 200 *μ*L, 50 pM *E. coli* SAH/MTA nucleosidase was incubated for 10 min at room temperature with 2.5 *μ*M MTA, and inhibitor ranging in concentration from 0.005 to 100 *μ*M. The reaction was terminated by the addition of 10 *μ*L of 8% TFA. Stopped assays were analyzed by RP-HPLC using a Zorbax 80A extend C8 column developed with TFA/AcCN/water mobile phase. Peaks corresponding to MTA were integrated, turnover calculated, and plotted to determine IC50 and *K*$_i$. A *K*$_m$ of 1.0 *μ*M for MTA and *E. coli* SAH/MTA nucleosidase was used to calculate *K*$_i$.

References

(1) (a) Della Ragione, F.; Porcelli, M.; Carteni-Farina, M.; Zappia, V.; Pegg, A. E. *Escherichia coli* S-Adenosylhomocysteine/5′-Methylthioadenosine Nucleosidase. *Biochem. J.* **1985**, *232*, 335−341. (b) Cornell, K. A.; Swarts, W. E.; Barry, R. D.; Riscoe, M. K. Characterization of Recombinant *Escherichia coli* S-Adenosylhomocysteine/5′-Methylthioadenosine Nucleosidase: Analysis of Enzymatic Activity and Substrate Specificity. *Biochem. Biophys. Res. Comm.* **1996**, *228*, 724−732. (c) Allart, B.; Gatel, M.; Guillerm, D.; Guillerm, G. The Catalytic Mechanism of Adenosylhomocysteine/Methylthioadenosine Nucleosidase from *Escherichia coli*. Chemical Evidence for a Transition State with a Substantial Oxocarbenium Character. *Eur. J. Biochem.* **1998**, *256*, 155−162. (d) Cornell, K. A.; Riscoe, M. K. Cloning and Expression of *Escherichia coli* 5′-Methylthioadenosine/S-Adenosylhomocysteine Nucleosidase: Identification of the *pfs* Gene Product. *Biochim. Biophys. Acta* **1998**, *1396*, 8−14. (e) Lee, J. E.; Cornell, K. A.; Riscoe, M. K.; Howell, P. L. Structure of *E. coli* 5′-Methylthioadenosine/S-Adenosylhomocysteine Nucleosidase Reveals Similarity to the Purine Nucleoside Phosphorylases. *Structure* **2001**, *9*, 941−953.

(2) Mao, C.; Cook, W. J.; Zhou, M.; Federov, A. A.; Almo, S. C.; Ealick, S. E. Calf spleen purine nucleoside phosphorylase complexed with substrates and substrate analogues. *Biochemistry* **1998**, *37*, 7135−46.

(3) Appleby, T. C.; Erion, M. D.; Ealick, S. E. The structure of human 5′-deoxy-5′-methylthioadenosine phosphorylase at 1.7 Å resolution provides insights into substrate binding and catalysis. *Struct. Fold Des.* **1999**, *7*, 629−41.

(4) (a) Surette, M. G.; Miller, M. B.; Bassler, B. L. Quorum Sensing in *Escherichia coli*, *Salmonella typhimurium*, and *Vibrio harveyi*: A New Family of Genes Responsible for Autoinducer Production. *Proc. Natl. Acad. Sci. U.S.A.* **1999**, *96*, 1639−1644. (b) Schauder, S.; Shokat, K.; Surette, M. G.; Bassler, B. L. The LuxS Family of Bacterial Autoinducers: Biosynthesis of a Novel Quorum-Sensing Signal Molecule. *Mol. Biol.* **2001**, *41*, 463−476.

(5) Lipinski, C. A.; Lombardo, F.; Dominy, B. W.; Feeney, P. F. Experimental and computational approaches to estimate solubility and permeability in drug discovery and development setting. *Adv. Drug Del. Rev.* **1997**, *23*, 3−25.

(6) V. Auwers, D. *Justus Lieb. Ann. Chem.* **1927**, *451*, 285−302.

(7) Bergman, J.; Bergman, S.; Brimert, T. *Tetrahedron* **1999**, *55*, 10447−10466.

(8) Cai, S. X.; Huang, J.-C.; Espitia, S. A.; Tran, M.; Ilyin, V. I.; Hawkinson, J. E.; Woodward, R. M.; Weber, E.; Keana, J. F. W. 5-(*N*-Oxyaza)-7-substituted-1,4-dihydroquinoxaline-2,3-diones: Novel, Systemically Active and Broad Spectrum Antagonists for NMDA/glycine, AMPA, and Kainate Receptors. *J. Med. Chem.* **1997**, *40*, 3679−3686.

(9) Abdel-Magid, A. F.; Carson, K. G.; Harris, B. D.; Maryanoff, C. A.; Rekha, D.; Shah, R. D. Reductive Amination of Aldehydes and Ketones with Sodium Triacetoxyborohydride. Studies on Direct and Indirect Reductive Amination Procedures. *J. Org. Chem.* **1996**, *61*, 3849−3862.

(10) (a) Hassan, J.; Sevignon, M.; Gozzi, C.; Schulz, E.; Lemaire, M. *Chem. Rev.* **2002**, *102*, 1359−1470. (b) Miyaura, N.; Suzuki, A. *Chem. Rev.* **1995**, 2457−2483.

(11) Koellner, G.; Luic, M.; Shugar, D.; Saenger, W.; Bzowska, A. Crystal structure of the tenary complex of *E. coli* purine nucleoside phosphorylase with formycin B, a structural analogue of the substrate inosine, and phosphate (Sulphate) at 2.1 Å resolution. *J. Mol. Biol.* **1998**, *280*, 153−166.

(12) Chambers, C. C.; Hawkins, G. D.; Cramer, C. J.; Truhlar, D. G. Model for aqueous solvation based on class IV atomic charges and first solvation shell effects. *J. Phys. Chem.* **1996**, *100*, 16385−16398.